JOURNAL OF APPLIED ELECTROCHEMISTRY 17 (1987) 1213–1222

Electro-oxidation rate of p-*tert-butyltoluene in a bipolar packed-bed electrode cell*

HARK JOON KIM*, KATSUKI KUSAKABE, SATOKO HOKAZONO, SHIGEHARU MOROOKA, YASUO KATO

Department of Applied Chemistry, Kyushu University, Higashi-ku, Fukuoka 812, Japan

Received 21 January 1987; revised 28 May 1987

The side chain methoxylation of *p*-tert-butyltoluene was carried out in a bipolar packed-bed electrode cell in which graphite pellets of diameter 4.74 mm and length 5 mm were randomly packed in nine layers separated by inert mesh spacers. The reaction consisted of main consecutive reactions leading to *p*-tert-butylbenzyl methyl ether and *p*-tert-butylbenzaldehyde dimethyl acetal (TBDA) and polymerization reactions. Overall reaction rate coefficients for each reaction step, current efficiency and energy consumption were determined on the basis of a reactor model. The selectivity and the current efficiency for TBDA increased with increasing current, but the energy consumption began to rise when the current exceeded 0.8 A. An addition of supporting electrolyte suppressed the overall reaction rate coefficients, although it decreased the energy consumption.

Nomenclature

C_e	overall current efficiency
C_i	concentration of i-component as a function of time. (i represents BT for TBT, ME for TBME and DA for TBDA) ($mol\,m^{-3}$)
E	cell voltage (V)
E_c	energy consumption ($J\,kg^{-1}$)
e	potential difference between upper and lower ends of each pellet (V)
e_d	decomposition voltage (V)
F	Faraday constant ($C\,mol^{-1}$)
I_b	bypass current (A)
I_p	faradaic current (A)
I_t	total current (A)
k_1, k_2, k_3	overall reaction rate coefficient, defined by Equation 13 ($m\,s^{-1}$)
M_i	molecular weight of i-component (i represents ME for TBME and DA for TBDA) ($kg\,mol^{-1}$)
n	number of pellet layers
R_b	equivalent resistance for bypass current (Ω)
R_p	equivalent resistance for faradaic current (Ω)
R_s	equivalent resistance for total current (i.e. spacer resistance) (Ω)
S	total surface area of anodic part of bipolarized pellets in cell (m^2)
t	time (s)
W	volume of electrolyte (m^3)
z	number of electrons transferred in electrochemical reaction
η	intrinsic current efficiency

Subscript

0	refers to initial values

1. Introduction

The electrochemical oxidation of alkylbenzenes is an attractive method for the synthesis of oxygen-containing aromatic components. Methoxylation of *p*-tert-butyltoluene is one of the most promising reactions [1–5]. Several researchers [2, 5–7] have reported that the side-chain oxidation occurs via nucleophilic attack of methanol on a benzyl cation formed by a deprotonation/anode oxidation

* On leave from Kyungnam University under the Korean Science and Engineering Foundation Overseas Fellowship scheme.

0021–891X/87 $03.00 + .12

process. However, detailed reaction kinetics and optimum electrolysis conditions are not fully understood. In addition, cell designs for efficient electrolysis require further investigation.

The bipolar packed-bed electrode (BPBE) cell is a useful novel reactor for large-scale electro-organic synthesis [8–12]. In the BPBE cell a number of particles are packed between two feeder electrodes and each particle works as a bipolar electrode when the terminal voltage of the BPBE cell is sufficiently high. Thus the distance between bipolar particles is of the order of 1 mm and the effective electrode area per unit cell volume becomes larger than $10\,cm^{-1}$. The simple configuration and operation are also attractive features of the BPBE cell.

In this study we investigate the electrochemical methoxylation of *p*-tert-butyltoluene (TBT) in methanol using a BPBE cell. Reaction kinetics, current efficiency and energy consumption are determined on the basis of the BPBE cell model.

2. Experimental apparatus and procedure

The construction of the BPBE cell used in this work is shown in Fig. 1, and is essentially the same as that used in previous work [11]. The centre compartment of the packed bed was made of a glass cylinder of diameter 7.5 cm and length 6 cm. Graphite pellets of diameter 4.74 mm and length 5 mm were packed into nine layers between the two perforated graphite plates used as the current feeders. These electrodes were made of #EG38 graphite plate supplied by Nippon Carbon Co., and about 175 pellets were packed in each layer. The cross-sectional area of the feeder electrodes was $44.2\,cm^2$ and the fraction of open area was 0.27. The total projected surface area of the pellets was $345\,cm^2$ which was roughly equal to the total anodic area of the bipolar pellets. The electrolyte was 350 ml in volume and was circulated by means of a roller pump between the cell and the cooling coil section dipped in a water bath. Electrolysis was carried out at constant current. The operating temperature was 308 K except for the case otherwise mentioned.

The concentrations of TBT and the products were determined periodically by means of gas chromatography with a separation column of polyethylene glycol-HT. The products were identified with gas chromatography/mass spectrometry, nuclear magnetic resonance and infrared spectroscopy. Higher molecular weight products composed of two or more benzene rings, however, were not identified in the present study.

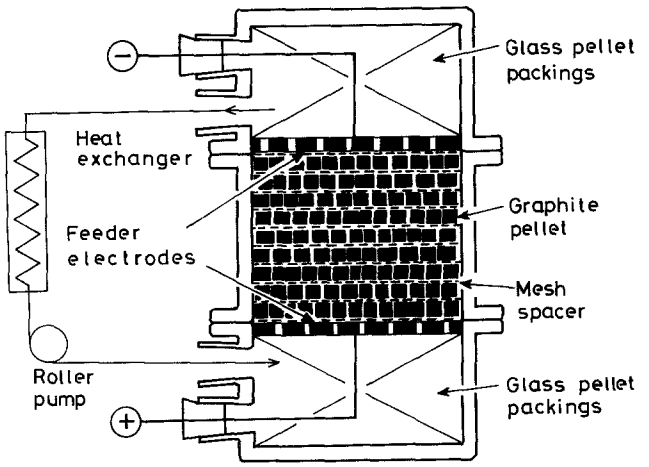

Fig. 1. Schematic view of bipolar packed-bed electrode cell.

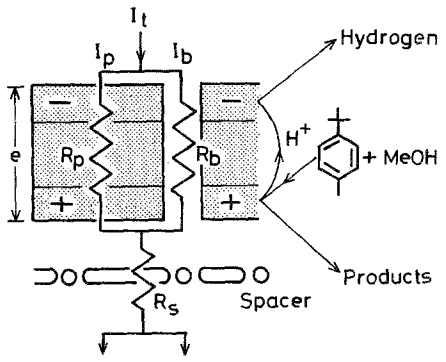

Fig. 2. Equivalent resistance model for current pathways.

3. Results and discussion

3.1. *Current pathways in the BPBE cell*

Fig. 2 illustrates the current pathways in a BPBE cell. The total current flowing through the open space of each insulation net consists of the faradaic and the bypass current,

$$I_t = I_p + I_b \tag{1}$$

Each current can be expressed by the equivalent resistance, i.e. R_s for I_t, R_p for I_p, and R_b for I_b.

Electrolysis may take place when the potential difference between the two sides of a graphite pellet, e, is larger than the decomposition voltage, e_d. Thus the faradaic current is

$$I_p = (e - e_d)/R_p \tag{2}$$

The potential difference is represented by

$$e = I_b R_b = (I_t - I_p)R_b \tag{3}$$

The number of working layers in the cell is considered to be $(n + 1)$, because the feeder electrode is also working. Thus the cell voltage is given by

$$E = (n + 1)(e + I_t R_s) \tag{4}$$

From Equations 1 to 4 we have

$$I_t = \frac{(R_p + R_b)E - (n + 1)R_b e_d}{(n + 1)(R_b R_p + R_p R_s + R_s R_b)} \tag{5}$$

$$I_b = \frac{R_p E + (n + 1)R_s e_d}{(n + 1)(R_b R_p + R_p R_s + R_s R_b)} \tag{6}$$

$$I_p = \frac{R_b E - (n + 1)(R_b + R_s)e_d}{(n + 1)(R_b R_p + R_p R_s + R_s R_b)} \tag{7}$$

The overall current efficiency based on I_t and the energy consumption are represented by

$$C_e = zFC_i W/(I_t t) \tag{8}$$

$$E_c = zFE/(C_e M_i) \tag{9}$$

The faradaic current flows through the packed layers in series in the BPBE cell. Then Equation 8 becomes

$$C_e = (I_p n + I_t)\eta/I_t \tag{10}$$

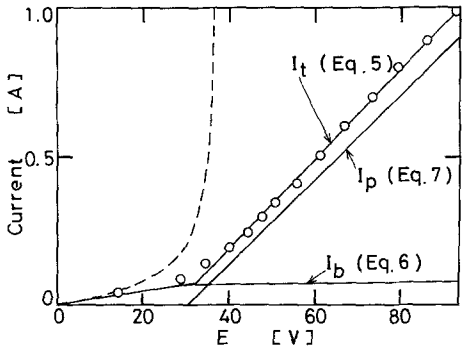

Fig. 3. Current–voltage curves for the bipolar packed-bed cell. Electrolyte, methanol–acetic acid (9 : 1) mixture containing 0.02 mol l^{-1} $NaBF_4$ and 0.08 mol l^{-1} TBT; electrolyte conductivity, 0.116 S m^{-1}; apparent resistance between current feeders, 56 Ω; temperature, 298 K.

where I_t in the numerator indicates the contribution of the feeder electrode, and η is the intrinsic current efficiency based on I_p. From Equations 4 to 10 we get

$$C_e = \frac{\{[(n+1)R_b + R_p]E - [(n+1)R_b + nR_s](n+1)e_d\}\eta}{E(R_p + R_b) - (n+1)e_d R_b} \tag{11}$$

Fig. 3 shows the cell voltage–current curves in the BPBE cell. The superficial decomposition voltage of TBT was about 2.7 V. The values of R_s and R_b were evaluated by the method of the previous paper [11] and were 5.5 Ω and 41.7 Ω in this case. Then R_p was calculated from Equation 5 as 1.1 Ω. The solid lines in Fig. 3 indicate the calculated values of I_t, I_b and I_p from Equations 5, 6 and 7, respectively. The ratio of the calculated faradaic current to the calculated bypass current in the fully bipolarized state was about 9.

3.2. *Reaction kinetics*

Fig. 4 illustrates cyclic voltammograms with and without TBT in methanol. Curves were obtained by using a graphite disc electrode, 4 mm in diameter, against a Ag/AgCl reference electrode. The addition of TBT diminishes the peak at about 1.3 V which is assigned to the oxidation of methanol. This means that TBT is oxidized at a lower anodic potential than methanol.

Fig. 5 shows typical changes in the concentrations of TBT and products as a function of time in a mixed solvent of methanol, acetic acid and sodium borofluoride. The anodic oxidation of TBT

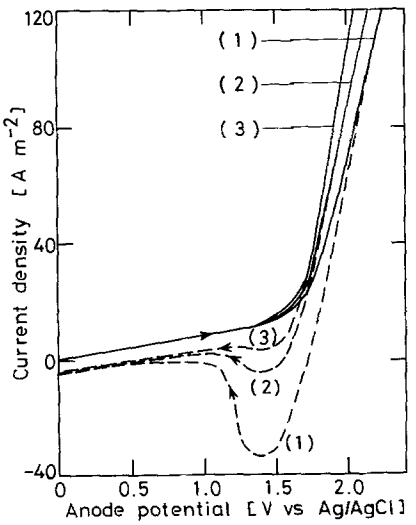

Fig. 4. Effect of C_{BT} on cyclic voltammograms. Electrolyte, methanol + 0.02 mol l^{-1} $NaBF_4$; scanning rate, 100 mV s^{-1}. TBT concentration: (1) 0 mol l^{-1}, (2) 0.012 mol l^{-1}, (3) 0.024 mol l^{-1}.

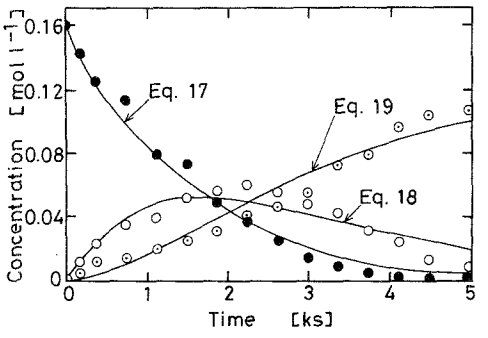

Fig. 5. Time-dependent changes in concentrations of TBT, TBME and TBDA. Electrolyte, methanol–acetic acid (9 : 1) mixture containing 0.01 mol l^{-1} $NaBF_4$ and 0.16 mol l^{-1} TBT; I_t, 0.8 A; flow rate, 14 ml s^{-1}.

proceeds via the consecutive side-chain methoxylation leading to *p*-t-butylbenzyl methyl ether (TBME) and *p*-t-butylbenzaldehyde dimethyl acetal (TBDA).

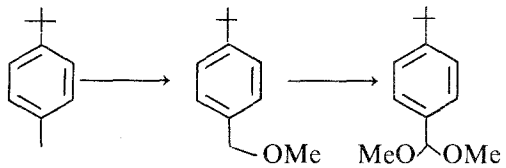

(TBT) (TBME) (TBDA) (12)

During the electrolysis, the solution was darkened due to tar and oligomers [7, 13]. These by-products of TBT are probably formed via coupling of TBT [14, 15]. Methanol was also oxidized to 1-1-dimethoxymethan (methylal) [16] and methyl acetate. Thus the main anode reactions are summarized by the following scheme:

$$\begin{aligned}
&\mathrm{TBT} \xrightarrow[k_1]{\overset{-2e,\,-2\mathrm{H}^+}{\mathrm{CH_3OH}}} \mathrm{TBME} \xrightarrow[k_2]{\overset{-2e,\,-2\mathrm{H}^+}{\mathrm{CH_3OH}}} \mathrm{TBDA}\\
&\quad\ \ \Big\downarrow{\scriptstyle k_3}\\
&\quad\ \ \text{tar, oligomers, etc.}\\
&\mathrm{CH_3OH} \xrightarrow[2\mathrm{CH_3OH}]{-2e,\,-2\mathrm{H}^+} \mathrm{CH_2(OCH_3)_2}\\
&\quad\ \ \Big\downarrow{\scriptstyle \overset{-2e,\,-2\mathrm{H}^+}{\mathrm{CH_3COOH}}}\\
&\quad\ \ \mathrm{CH_3COOCH_3}
\end{aligned} \tag{13}$$

The overall reaction rate coefficient of the i-component, k_i, depends on current intensity as well as the adsorption of each component on the anode surface and chemical reactions near the electrode. The electron transfer step may not be rate determining [2].

If we assume

(i) mass transport resistance is negligible;

(ii) each reaction obeys irreversible first order kinetics with respect to its reactant concentration;

(iii) the reactor is a batch stirred tank,

we can describe the time-dependent changes of each component as follows:

$$-\mathrm{d}C_{\mathrm{BT}}/\mathrm{d}t = (k_1 + k_3)(S/W)C_{\mathrm{BT}} \tag{14}$$

$$\mathrm{d}C_{\mathrm{ME}}/\mathrm{d}t = [k_1 C_{\mathrm{BT}} - k_2 C_{\mathrm{ME}}](S/W) \tag{15}$$

$$\mathrm{d}C_{\mathrm{DA}}/\mathrm{d}t = k_2(S/W)C_{\mathrm{ME}} \tag{16}$$

where S is approximated by the sum of the total projected area of the pellets and the feeder anode. Equations 14 to 16 are integrated with the initial condition that the concentrations of TBME and TBDA are zero.

Table 1. Yield and current efficiency of TBDA with different electrolyte solutions[a]

Run	Solvent	Supporting electrolyte[b]	C_{BT} (mol l^{-1})	I_t (A)	E (V)	Charge passed (F mol^{-1})	Yield of TBDA (–)		k_2/k_1	k_3/k_1
							Chemical	Current[e]		
1	MeOH	H_2SO_4	0.08	0.8	53–57	1.0	0.49	2.0	1.1	0.4
2	MeOH	$NaBF_4$	0.08	0.8	71–88	0.89	0.52	2.3	2.3	0.9
3	MeOH	$NaBF_4$	0.16	0.8	73–96	0.93	0.57	2.8	1.7	0.8
4	MeOH–AcOH[c]	H_2SO_4	0.02	0.5	74–81	2.22	0.47	0.7	3.0	2.4
5	MeOH–AcOH[c]	$LiBF_4$	0.04	0.5	55–66	1.33	0.47	1.4	1.6	0.6
6	MeOH–AcOH[c]	$NaBF_4$	0.04	0.5	58–65	1.33	0.55	1.6	1.5	0.1
7	MeOH–AcOH[c]	$NaBF_4$	0.08	0.8	70–79	0.89	0.54	2.4	1.2	0.1
8	MeOH–AcOH[c]	$NaBF_4$	0.16	0.8	72–86	0.93	0.68	3.3	1.2	0.2
9	MeOH–AcOH–H_2O[d]	$NaBF_4$	0.16	0.8	73–101	0.93	0.26	1.1	1.3	1.3

[a] Temperature, 308 K; circulation flow rate, 14 ml s^{-1}. [b] Concentration, 0.02 mol l^{-1} except for run 4 (0.01 mol l^{-1}); conductivity, 0.13–0.17 S m^{-1}. [c] Methanol: AcOH = 9 : 1 (by volume). [d] Water content, 5 vol %.

$$C_{BT} = C_{BT0} \exp [-(k_1 + k_3)tS/W] \quad (17)$$

$$C_{ME} = C_{BT0}k_1\{\exp [-(k_1 + k_3)tS/W] - \exp [-k_2tS/W]\}/(k_2 - k_1 - k_3) \quad (18)$$

$$C_{DA} = C_{BT0}k_1\{k_2/(k_1 + k_3)[1 - \exp (-k_1 - k_3)tS/W] - [1 - \exp (-k_2tS/W)]\}/(k_2 - k_1 - k_3) \quad (19)$$

The overall reaction rate coefficients, k_1, k_2 and k_3, are determined by comparing Equations 17 to 19 with experimental data by means of the non-linear least-squares method.

Table 1 shows the effects of electrolysis conditions on the yield and selectivity of TBDA. The co-solvent of acetic acid increases the current efficiency of TBDA, although it promotes the formation of methyl acetate. Active methoxy radicals which are generated preferentially at lower anode potentials are scavenged by acetic acid and are converted into methyl acetate. Then the nucleophilic attack of methoxy radicals on the benzene nucleus is retarded. The electrolysis in methanol/acetic acid solution containing $NaBF_4$ is superior to that of other electrolytes such as sulphuric acid and sodium *p*-toluenesulphonate. This condition gives a large value of k_1 and a small value of k_3/k_1. The addition of water reduces the current efficiency for the side chain oxidation of TBT and promotes the formation of tar and oligomers.

Fig. 6 shows that the current efficiency of TBDA and the selectivity of TBDA increase when the total cell current (consequently the anode potential) increases. The overall reaction rate coefficients calculated from these data are plotted in Fig. 7. The values of k_1 and k_2 are not proportional to the current intensity because the current efficiency declines with an increase in I_t. It is evident that the formation of TBME and TBDA is favourable at higher anode potentials. The change in the ratio of bypass current to total current agrees well with Equations 5 and 7.

The effect of $NaBF_4$ concentration on the overall reaction rate coefficients is shown in Table 2 and Fig. 8. An excessive addition of $NaBF_4$ increases the electrolyte conductivity and consequently decreases the potential gradient in the cell under the condition of constant current operation. This causes a loss of the effective anode area [9]. On the other hand, the addition of $NaBF_4$ reduces the energy consumption in the spacer region.

As indicated in Fig. 9, the lower electrolyte temperature results in the higher selectivity of TBDA. Fig. 10 is the Arrhenius plot of the overall reaction coefficients. The value of k_1 increases with increasing reaction temperature, but k_2 and k_3 decrease.

Fig. 11 shows the effect of the electrolysis current on the overall current efficiency, the intrinsic current efficiency per unit layer of pellets and the energy consumption for TBDA production. The

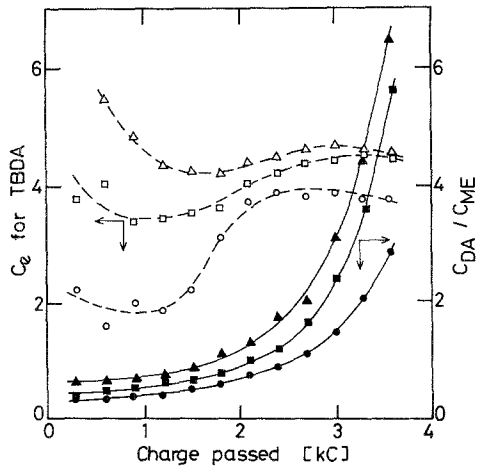

Fig. 6. Variations of current efficiency and C_{DA}/C_{ME}. Electrolyte, methanol–acetic acid (9:1) mixture containing 0.02 mol l^{-1} $NaBF_4$ and 0.16 mol l^{-1} TBT; flow rate, 14 ml s^{-1}. Values of I_t: (○, ●) 0.5 A; (□, ■) 0.8 A; (△, ▲) 1.2 A.

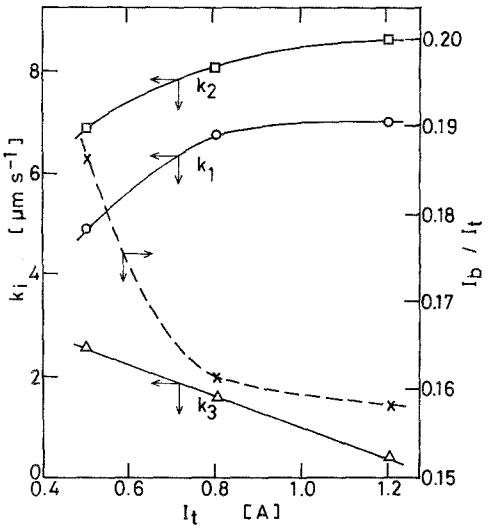

Fig. 7. Effect of I_t on overall reaction rate coefficients and bypass current fraction. Electrolysis conditions as in Fig. 6. ○ = k_1; □ = k_2; △ = k_3; × = I_b/I_t.

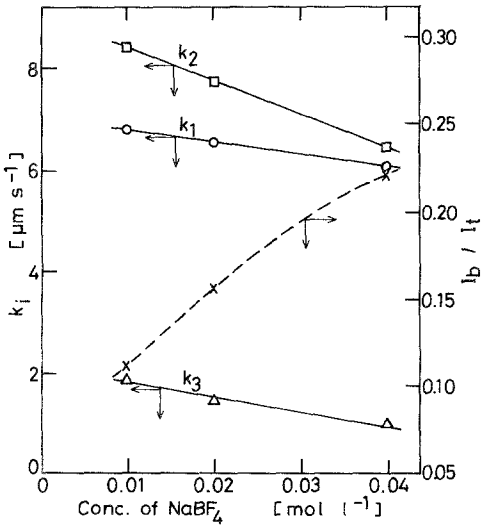

Fig. 8. Effects of $NaBF_4$ concentration on overall reaction rate coefficients and bypass current fraction. Electrolyte conditions as in Table 2. ○ = k_1; □ = k_2; △ = k_3; × = I_b/I_t.

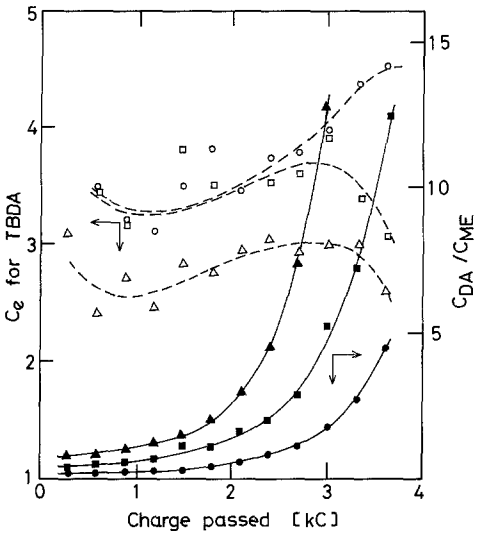

Fig. 9. Variations of current efficiency and C_{DA}/C_{ME} with temperature. $I_t = 0.8$ A; other conditions are the same as in Fig. 6. (△, ▲) 263 K, (□, ■) 289 K; (○●) 308 K.

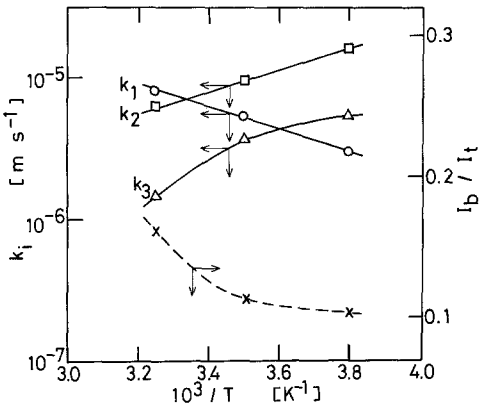

Fig. 10. Effect of temperature on overall reaction rate coefficients and bypass current fraction. Electrolysis conditions as in Fig. 9. ○ = k_1; □ = k_2; △ = k_3; × = I_b/I_t.

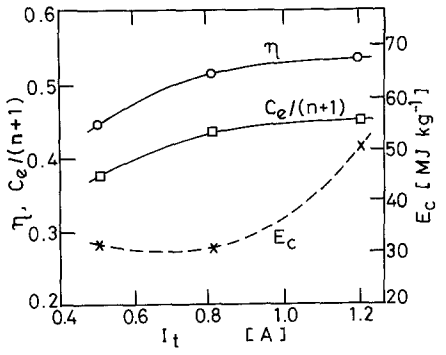

Fig. 11. Effect of I_t on current efficiency, intrinsic current efficiency and energy consumption. Charge passed, 0.56 F mol^{-1}; other conditions as in Fig. 6.

Table 2. Yield and current efficiency of TBDA with different concentrations of supporting electrolyte[a]

Supporting electrolyte ($mol\,l^{-1}$)	*Conductivity* ($S\,m^{-1}$)	*E* (V)	*Yield of TBDA (–)*		E_c ($MJ\,kg^{-1}$)
			Chemical	*Current*[b]	
0.01	0.079	112–164	0.82	4.8	53.6
0.02	0.145	73–83	0.79	4.6	31.0
0.04	0.245	60–62	0.72	3.9	29.2

[a] Electrolyte solution, 0.16 M TBT–$NaBF_4$–MeOH–AcOH; MeOH : AcOH = 9 : 1 (by volume). Circulation flow rate, $14\,ml\,s^{-1}$. Total current, 0.8 A. Charge passed, $0.67\,F\,mol^{-1}$. Conversion of TBT, 0.98–0.99. [b] Equation (8).

Table 3. Yield and current efficiency of TBDA with different circulation flow rate[a]

Flow rate ($ml\,s^{-1}$)	*E* (V)	*Yield of TBDA (–)*		E_c ($MJ\,kg^{-1}$)
		Chemical	*Current*[b]	
2.2	72–85	0.67	3.9	38.5
14	71–82	0.81	4.3	32.7
26	68–82	0.84	4.5	30.7

[a] Electrolyte solution, MeOH–AcOH (9 : 1 by volume) added with TBT ($0.16\,mol\,l^{-1}$) and $NaBF_4$ ($0.02\,mol\,l^{-1}$); temperature, 308 K; total current, 0.8 A; charge passed, $0.74\,F\,mol^{-1}$; conversion of TBT, 0.99. [b] Equation 8.

intrinsic current efficiency calculated from the faradaic current is 1.2 times larger than $C_e/(n + 1)$ based on the total current. The energy consumption begins to rise when I_t exceeds 0.8–1 A.

Table 3 describes the effect of electrolyte flow rate on the current efficiency and the energy consumption of TBDA. Hydrogen bubbles evolved in the cell must be entrained with the liquid flow. The current efficiency increases and the energy consumption decreases with increasing circulation rate.

4. Conclusion

Under constant current conditions, the selectivity and the current efficiency for the methoxylation of TBT in a BPBE cell increases with increasing total current, but the energy consumption begins to rise in the range $I_t > 0.8$ A. An excessive addition of $NaBF_4$ lowers k_1, k_2 and k_3. The value of k_1 for the formation of TBME is promoted at higher reaction temperatures while k_2 and k_3 are suppressed.

Thus electrochemical reaction steps are distinguished from current pathways which are important factors for cell designs. The present procedure can be applied to analyse the performance of other electro-organic reactions in a bipolar packed-bed electrode cell.

References

[1] P. Tissot, H. Do Duc and O. John, *J. Appl. Electrochem.* **11** (1981) 473.
[2] A. Nilsson, U. Palmquist, T. Pettersson and A. Ronlan, *J. Chem. Soc. Perkin Trans. I* (1978) 708.
[3] I. Nishiguchi and T. Hirasima, *J. Org. Chem.* **50** (1985) 539.
[4] K. Okumura, H. Mizumoto and H. Sasaki, *Jpn. Kokai Tokyo Koho* (1981) 81.
[5] S. Torii and T. Siroi, *J. Synth. Org. Chem. Jpn.* **37** (1979) 914.
[6] F. Barba, A. Guirado and I. Barba, *Electrochim. Acta* **29** (1984) 1639.
[7] N. L. Weinberg and H. R. Weinberg, *Chem. Rev.* **68** (1968) 449.
[8] F. Goodridge, C. J. H. King and A. R. Wright, *Electrochim. Acta.* **22** (1977) 347.

[9] K. Kusakabe, T. Kimura, S. Morooka and Y. Kato, *J. Chem. Eng. Jpn.* **17** (1984) 239.
[10] K. Kusakabe, S. Morooka and Y. Kato, *ibid.* **15** (1982) 45.
[11] *Idem. ibid.* **19** (1986) 43.
[12] S. Ehdaie, M. Fleischmann and R. E. W. Jansson, *J. Appl. Electrochem.* **12** (1982) 59.
[13] O. R. Brown, S. Chandra and J. A. Harrison, *J. Electroanal. Chem.* **34** (1972) 505.
[14] H. Sternerup, *Acta Chim. Scand.* **27** (1974) 579.
[15] S. Vemura, T. Ikeda, S. Tanaka and M. Okano, *J. Chem. Soc. Perkin Trans. I*, (1979) 2574.
[16] G. Sundholm, *J. Electroanal. Chem.* **31** (1971) 265.